Fatigue Behavior of Continuous Composite Beams

J. HARTLEY DANIELS and JOHN W. FISHER, Fritz Engineering Laboratory, Lehigh University

The provisions of the current (1965) AASHO Bridge Design Specifications for composite steel-concrete bridge beams are based on static tests and allow the omission of shear connectors in the negative moment regions of continuous composite beams which have continuous longitudinal slab reinforcement. The fatigue strength of shear connectors is not considered in these specifications. This was evaluated in a recent study where design recommendations were suggested which would provide adequate static and fatigue strength of the shear connectors in composite beams. It was also suggested that shear connectors are required in the negative moment regions of continuous composite beams which have continuous longitudinal slab reinforcement.

An experimental program was undertaken to evaluate the proposed design recommendations. Fatigue tests of 4 two-span full-size continuous composite beams were carried out to investigate the effect of shear connectors and variable amounts of longitudinal slab reinforcement in the negative moment region. It was concluded that shear connectors are required in the negative moment regions if satisfactory fatigue behavior is to be achieved. The study also indicated that more longitudinal reinforcement is required in the negative moment region than currently allowed by AASHO specifications to improve interaction and to better control slab cracking. The tests showed that a spreading of connectors is permissible in the vicinity of the maximum negative moments so that the tension flange stress near a connector does not control the design.

Further study is required to evaluate the effects of stud placement, cover plates, prestressing and haunching in the negative moment regions of continuous composite beams as well as to determine the optimum reinforcement required for adequate crack control.

•THE present specifications (1) for the design of shear connectors in composite steel-concrete bridge members are based on the static properties of the connectors (2). Hence, they note only that in the negative moment regions of continuous beams the slab reinforcement may be considered as contributing to the moment resisting capacity of a section if connectors are used. If connectors are provided only in the positive moment regions the specifications require that the steel beams be designed to resist the full negative moment.

Since design procedures based on the static properties of connectors have led to very conservative designs, no apparent difficulties have been encountered. In fact, fatigue tests of simple beams which were designed using criteria suggested elsewhere (1) have shown that adequate connector fatigue strength is available. The same was

Paper sponsored by Committee on Steel Superstructures and presented at the 47th Annual Meeting.

also assumed to be true for continuous beams. Because bridge engineers have recognized that such a design procedure is conservative, the factor of safety has been reduced in the present specifications (1). However, a recent study (3) has shown that it is not possible to reduce arbitrarily the factor of safety because the fatigue behavior may then become critical. Due to this apparent divergence in views, it was considered desirable to evaluate the performance of continuous composite beams with shear connectors proportioned using the design procedures suggested by Slutter and Fisher (3). The design criteria were based on the results of previous fatigue tests of simple-span composite beams (4, 5, 6) and on a fatigue test program which involved several factorial experiments on stud and channel shear connectors. In addition, both the fatigue and static behavior required further study and evaluation to determine the applicability of the suggested design procedures for continuous composite bridge members (3).

All previous studies on continuous composite beams have evaluated only their static behavior. Viest, Fountain, and Siess (2) discussed the negative moment regions of continuous composite beams in some detail. Their discussion was based on the static behavior of two composite model bridges reported by Siess and Viest (7). These two models differed in that one had shear connectors throughout the beam; the other had shear connectors in the positive moment regions only. They concluded that (a) in the negative moment regions only the longitudinal slab reinforcement can act compositely with the steel beam; (b) where shear connectors are used throughout a beam the longitudinal slab reinforcement is fully effective and when connectors are omitted from the negative moment region the slab reinforcement is only partly effective; and (c) the action of both continuous composite model bridges was about the same since the distribution of strains, and thus also of moments, in both the positive and negative moment regions was nearly the same. They also concluded that the use of an elastic analysis in combination with the usual load distribution factors is justified, and that no special provisions are needed for the design of continuous composite bridges (2).

Slutter and Driscoll (9) summarized the behavior of a single continuous composite beam tested statically to its ultimate load. They noted that the theoretical plastic collapse load was exceeded in the test even though the beam had inadequate shear connection throughout its length.

Barnard and Johnson (10) presented the results of a study on the plastic behavior of continuous composite beams. These preliminary studies were followed up by further ~~studies were followed up by~~ further studies designed to provide more information on secondary failures (11). In particular, the effects of cracking and transverse bending of the slab on the plastic behavior and the behavior of the longitudinal reinforcement in the negative moment regions were examined, but under static ultimate loads.

To provide experimental data on the fatigue strength of continuous composite beams having stud shear connectors in the negative moment region, comparative laboratory fatigue tests were conducted at Lehigh University on 4 full-size two-span continuous composite beams. Two of the beams were identical except that one had connectors in the negative moment region and the other did not, as is common practice in current designs. Both test beams had identical longitudinal and transverse reinforcement. The amount of reinforcement provided was made equal to that required by the present specifications (2, 8) for a bridge deck of similar proportions and subjected to H20-S16 truck loading. The other two continuous composite beams were similar to the first pair but had connectors throughout their length in addition to substantially more longitudinal reinforcement through their negative moment regions. This paper presents the results of the fatigue test program.

After the fatigue test program was completed, the 4 continuous composite beams were tested statically to their ultimate load capacity. The results of the static tests of these beams were reported elsewhere (12).

DESCRIPTION OF TEST BEAMS, INSTRUMENTATION, AND TEST PROCEDURE

Each of the 4 continuous composite beams which was fatigue tested was 50 ft long and had two equal spans of 25 ft between supports. Symmetrical concentrated pulsating loads, distributed transversely across the slab width, were placed 10 ft from the exterior

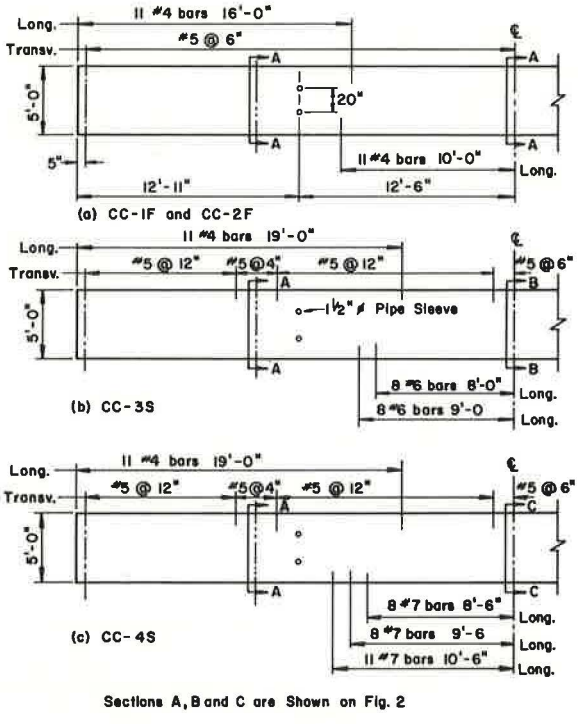

Figure 1. Details of composite beams.

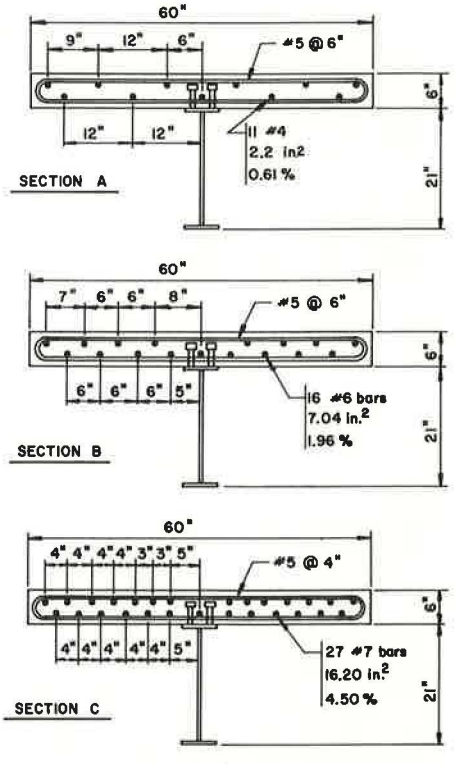

Figure 2. Typical cross-sections of test beams.

supports in each span. Each beam consisted of a reinforced concrete slab 60 in. wide and 6 in. thick connected to a 21W62 steel beam by pairs of $\frac{3}{4}$ in. x 4 in. headed steel stud shear connectors. The transverse spacing of studs in each stud pair was 4 in. The rolled beams were all supplied from the same heat of A36 steel. The four test beams were designated CC-1F, CC-2F, CC-3S, and CC-4S. Details of the test beams are shown in Figures 1 and 2.

Design Criteria

The composite beams were designed according to the transformed moment of inertia method by transforming the concrete slab to an equivalent area of steel in the positive moment regions using an assumed modular ratio of 10. The longitudinal reinforcing steel was considered in both the positive and negative moment regions. For purposes of this paper, the dead load point of inflection will define the positive and negative moment regions. Table 1 summarizes the resulting design stresses for the composite beams. A small spreading of shear connectors was made over the interior support of beam CC-2F so that the tensile stress in the beam flange adjacent to a stud shear connector did not exceed the specification value (1).

The longitudinal and transverse reinforcement for beams CC-1F and CC-2F was designed in accordance with the AASHO Bridge Specifications (1). The transverse reinforcing steel was designed assuming that an H20-S16 truck was placed on a 6-in. deck spanning 5 ft center-to-center of the steel beams. The longitudinal distribution reinforcement was made continuous and was taken as 0.67 percent of the required transverse reinforcement. The reinforcement for beams CC-3S and CC-4S was essentially the same except that the amount of transverse reinforcement was reduced by nearly one-half and the amount of longitudinal reinforcement through the negative moment regions was substantially increased. The longitudinal reinforcement in the positive moment regions of these two beams (except adjacent to the negative moment region)

TABLE 1

SUMMARY OF DESIGN STRESSES

Test Beam No.	Load		Flexural Stress (DL + LL)								Fatigue Life (10^6 cyc)	Stud Force (LL)[a]		
			At Load Points				At Center Support							
	Live (k)	Dead (k/ft)	WF Btm. (ksi)	WF Top (ksi)	Reinf. (ksi)	Conc. (ksi)	WF Btm. (ksi)	WF Top (ksi)	Reinf. (ksi)	Conc. (ksi)		Ext. Pos. Mom. (k)	Int. Pos. Mom. (k)	Neg. Mom. (k)
CC-1F	60	0.44	+20.7	-3.3	-5.5	-0.8	-19.2	+19.2	0[b]	0	2.0	4.4	4.4	—
CC-2F	60	0.44	+20.1	-3.3	-5.4	-0.7	-18.8	+15.3[c]	+17.2	0	2.0	4.4	4.4	4.4
CC-3S	60	0.44	+18.9	-2.9	-5.0	-0.6	-21.1	+11.7	+21.8	0	0.5	5.4	5.2	6.2
CC-4S	70	0.44	+22.0	-3.4	-5.9	-0.8	-21.8	+ 7.8	+24.6	0	0.5	6.1	6.4	4.3

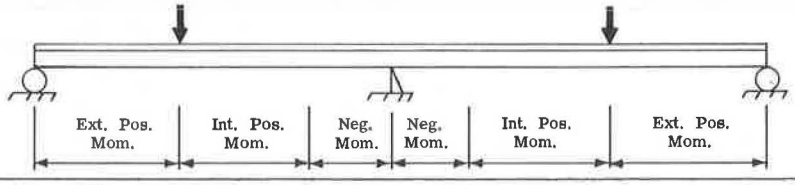

[a] Allowable force: 4.4 kips (2 x 10^6 cyc) or 5.94 kips (0.5 x 10^6 cyc), (3).
[b] Stress in reinforcement was neglected.
[c] Stress adjacent to nearest stud: 10.6 ksi.

was the same as in beams CC-1F and CC-2F. In CC-4S, the longitudinal reinforcement in the negative moment region was determined on the basis that the ultimate moment capacities of cross sections in the positive and negative moment regions would be nearly equal, using handbook properties. In beam CC-3S, the longitudinal reinforcement in the negative moment region was determined so that the ultimate moment capacity would be about midway between that for beams CC-2F and CC-4S.

The shear connectors in all 4 test beams were designed according to either the fatigue or static criteria proposed previously (3). For beams CC-1F and CC-2F, the connectors were proportioned to sustain a fatigue loading to 2,000, 000 cycles of zero to maximum load application (stress range = maximum stress). The two beams differed only in that connectors were not provided in the negative moment region of beam CC-1F. For beams CC-3S and CC-4S, the connectors were proportioned on the basis of the static strength requirements but were subjected to 500,000 cycles of zero to maximum load application. Consequently, only a certain number of the connectors in beams CC-3S and CC-4S were subjected to a range of shear near the suggested value (1, 3). Table 1 gives the expected forces on the shear connectors and indicates the critical regions in beams CC-3S and CC-4S.

Design Details and Fabrication

The details of the steel beams and connectors are shown in Figure 3. Each beam was cut from nominal length 57-ft rolled sections. The excess pieces were delivered to the laboratory after all shear connectors were installed to provide material for tension tests of the steel section and studs. The bearing stiffeners at the center supports of CC-1F and CC-2F were designed short to eliminate welds near the region of high tensile stresses. Web stiffeners and additional short bearing plates in the region of the center supports of beams CC-3S and CC-4S were installed in the laboratory to stiffen that region and to prevent premature failure of the beams during the static ultimate load tests.

All studs were placed in pairs except in the negative moment region of beam CC-2F where single studs were staggered (Fig. 3). Before the studs were welded to the test beams, the welding equipment was calibrated by welding several studs to the excess lengths that were cut off. The quality of the welds was verified using the welding and inspection procedure outlined elswhere (13). Two different lots of studs, supplied by two manufacturers, were installed. Beams CC-1F and CC-4S had lot A studs, and beams CC-2F and CC-3S had lot B studs. This choice was random.

The placement of reinforcing bars is shown in Figures 1 and 2. The lapped No. 4 bars in CC-1F and CC-2F were welded to provide continuous longitudinal reinforcement throughout. No welding was done in beams CC-3S and CC-4S.

The transverse reinforcement in all beams was provided by No.5 bars bent into rectangular hoops. In beams CC-1F and CC-2F, these bars were placed on 6-in. centers throughout the beam. For beams CC-3S and CC-4S, a variable spacing was used (Fig. 1). The crack patterns and test results for beams CC-1F and CC-2F indicated that it was not necessary to provide such a large amount of transverse reinforcing steel in most of the positive and negative moment regions since longitudinal cracking of the slab was not a factor. However, a closer spacing was used under the load points and at the center support to provide for cross bending of the slab at these points.

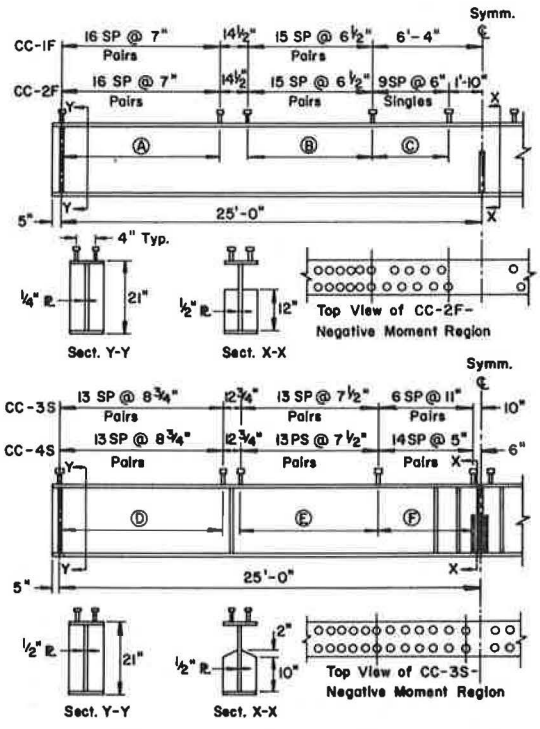

Figure 3. Details of steel beams.

Construction

Construction of the continuous composite T-beams began with the erection of a pair of the steel beams on supports bolted to the dynamic test bed in the laboratory. The beams were spaced 5 ft 2 in. apart and clamped to the supports. Plywood forms for the slabs of the two T-beams were suspended from the beams. A 2-in. timber spacer was used to separate the slabs of the two T-beams along their length.

The slabs were made with transit-mixed concrete proportioned for a 28-day compressive strength of 3,000 psi. Beams CC-1F and CC-2F were constructed first. The concrete placement began simultaneously at the exterior supports of each span and progressed toward the interior supports. Placement was stopped 6 ft on either side of the interior supports. The remaining 12 ft was placed a week later to allow time for installation of strain gages on the reinforcement in that region. Beams CC-3S and CC-4S were constructed later and the concrete placement began at one exterior support and progressed to the other end. Consolidation was accomplished by internal vibration along the slab as placement progressed. The final finish was obtained by hand troweling. From 16 to 32 test cylinders were poured with each placement.

The concrete in the slabs of all beams was moist-cured for 7 days with the exposed surface covered with wet burlap and a polyethylene sheet. The forms for each pair of test specimens were removed approximately 14 days after casting, then the specimens were allowed to cure under dry conditions for at least 14 days.

The mechanical properties of the structural steel beams were determined from tests of tensile coupons cut from a 2-ft piece of the beam that had been flame cut from the original 57-ft length. The coupons were tested in tension at a speed of 0.025 in./min up to the onset of strain hardening and then at a speed of 0.50 in. min to fracture. The mean values and standard deviation of the yield point, static yield stress, and the ultimate strength are given in Table 2. Values of the modulus of elasticity and the strain hardening modulus are also given.

The mechanical properties of the Nos. 4, 6, and 7 deformed longitudinal reinforcing bars were determined by tension tests of 3-ft lengths of reinforcement. The deformed bars were of intermediate grade steel conforming to ASTM A15. The average yield points and ultimate strengths are also given in Table 2.

TABLE 2

MATERIAL PROPERTIES OF STEEL

Type of Specimen	No. of Tests	Yield Point[a] (ksi)		Static Yield Stress (ksi)		Tensile Strength (ksi)	
		Mean	Std. Dev.	Mean	Std. Dev.	Mean	Std. Dev.
Web[b] (21WF62)	12	37.3	2.24	35.0	2.19	62.1	2.26
Flange[b] (21WF62)	12	36.4	0.81	34.3	0.85	61.6	0.87
No. 4 Bar	2	50.1	—	47.9	—	78.4	—
No. 6 Bar	2	45.1	—	43.0	—	75.2	—
No. 7 Bar	2	46.7	—	44.4	—	78.2	—
¾ In. Studs A	5	54.9	—	—	—	70.4	1.86
¾ In. Studs B	5	62.3	—	—	—	73.3	1.76

[a] Yield point applies to 21WF62 only; other values refer to yield strength at 2 percent offset.
[b] Average modulus of elasticity $E = 30.1 \times 10^3$ (ksi); average strain hardening modulus $E_{st} = 0.685 \times 10^3$ (ksi).

The properties of the studs were determined from tensile tests on full-size studs. The average yield points and ultimate strengths are summarized in Table 2.

The concrete placed in the slabs of all four beams was made of Type 1 portland cement, crushed gravel, and natural bank sand. The standard 6 by 12-in. cylinders poured during slab casting were tested at 28 days and at the beginning of each fatigue test. The 28-day cylinders were moist cured. The other cylinders were cured under approximately the same curing conditions as the slabs. The compressive strengths, splitting strengths, and moduli of elasticity are given in Table 3.

Actual Cross-Section Properties

The section properties of the composite sections in the positive moment regions were computed assuming that the effective width of the slab was the full 5-ft width, and that the modulus of elasticity of the concrete was equal to that determined from the 28-day cylinder tests. The section properties of the composite sections in the negative moment regions were computed based on the steel beam and the longitudinal reinforcing steel. It was assumed that the concrete slab was cracked throughout. Table 4 gives the values of the moments of inertia and the distance of the neutral axis from the bottom of the beam for each test beam.

TABLE 3

RESULTS OF CONCRETE CYLINDER TESTS

Beam	Location	Moist Cured						Dry Cured			
		No. of Tests	Age (days)	Splitting Tensile Strength, T (psi)		Compressive Strength, f'_c (psi)		Modulus of Elasticity ($\times 10^3$ ksi)	No. of Tests	Age (days)	Compressive Strength, f'_c (psi)	
				Mean	Std. Dev.	Mean	Std. Dev.				Mean	Std. Dev.
CC-1F and CC-2F	Positive moment	4	28	550	28.1	5164	462.7	3.85	12	35 to 84	5602	319.9
CC-1F and CC-2F	Negative moment	6	28	564	68.0	5247	213.2	3.85	9	37 to 78	5611	98.8
CC-3S and CC-4S	Positive and negative moment	7	28	432	2.55	3581	116.0	3.57	9	93	3964	131.1

Note: The 3,000-psi mix design for beams CC-1F and CC-2F gave substantially higher strengths; the mix was altered for beams CC-3S and CC-4S to obtain a reduced strength.

Instrumentation

The instrumentation for beams CC-1F and CC-2F was essentially the same. The instrumentation for beams CC-3S and CC-4S was also essentially the same but differed from that for the first two beams. A combination of electrical resistance strain gages, dial gages, and level bars was used.

Figure 4 shows the location of the strain gages used to determine the flexural strains in the steel beams and in the concrete slabs. These gages were used to ascertain the transverse distribution of the strain during the fatigue test. Strain gages were also attached to the top surface of all the longitudinal No. 4 bars at the cross-section containing the interior support.

Figure 5(a) shows the location of the studs which had strain gages mounted under them on the bottom of the top flange. Figure 5(b) shows the placement of these gages relative to a stud. The strain gage is not placed directly under a stud but offset slightly in the direction of the expected shear force on the stud. No significance is attached to the absolute magnitude of measured strain. However, relative values of measured strain serve to indicate the relative magnitudes of the shear force being transmitted by the stud above the strain gage. Their use and development have been discussed in detail (4, 5).

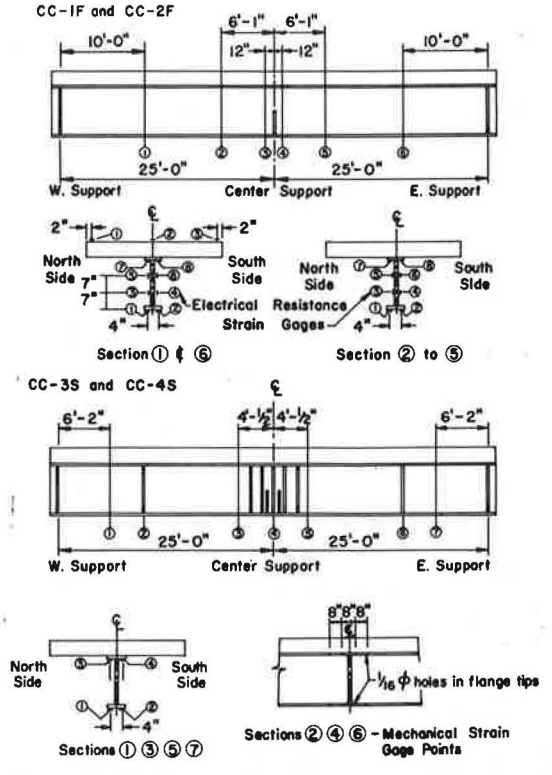

Figure 4. Strain gage locations on steel beams and concrete slabs.

Dial gages (0.001 in.) were placed under the beams at the load points to measure vertical deflection. These gage readings were used to adjust the maximum dynamic load level at the beginning and throughout the duration of each beam test. Dial gages (0.001 in.) were also used to measure slip at each end of the beams and at various sections along the beam spans.

For beams CC-3S and CC-4S, a large compression dynamometer was used at the interior support to measure the center reaction. This reaction was used together with the known loads to determine bending moments along the beam. A check was thus provided on the bending moments computed from the strain measurements on the steel beam.

A 40-power microscope was used to measure the width of cracks in the slab in the negative moment region of CC-3S. Crack widths during the other three beam tests were estimated. In addition, the crack patterns were photographed following each beam test.

TABLE 4

PROPERTIES OF COMPOSITE BEAMS

Beam	Positive Moment Regions		Negative Moment Regions	
	Moment of Inertia ($in.^4$)	Position of Neutral Axis from Bottom (in.)	Moment of Inertia ($in.^4$)	Position Neutral Axis from Bottom (in.)
CC-1F	3661	19.35	1348	10.50
CC-2F	3600	19.35	1662	11.90
CC-3S	3584	19.45	2198	14.25
CC-4S	3594	19.45	2851	16.90

Test Procedure

A pulsating concentrated load was applied simultaneously to each span by hydraulic jacks. The loading rate was constant for all beams at 250 cycles of zero to maximum load per minute. The test setups are shown in Figure 6. The interior support of CC-1F and CC-2F consisted of a bearing plate free to rotate on a fixed support assembly. Longitudinal and lateral stability was thus provided at this point. For beams

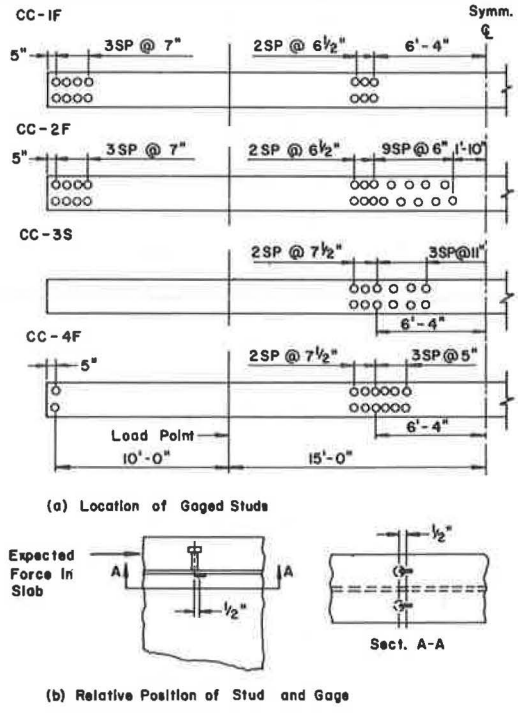

Figure 5. Location of gaged studs and position of strain gages under studs.

CC-3S and CC-4S the interior support was replaced by a bearing plate resting on a compression dynamometer, which provided no longitudinal or lateral stability to the beam. A supplementary support assembly was used to provide horizontal support at this point.

Fatigue testing of beams CC-1F, CC-2F, CC-3S, and CC-4S was started 35, 71, 39, and 45 days, respectively, after the concrete slabs were cast. Prior to any fatigue loading, each beam was loaded once, statically, to the maximum load to be applied during the fatigue test. This load was applied in increments of 10 kips up to a maximum of 60 kips at each load point for beams CC-1F, CC-2F, and CC-3S and up to 70 kips for beam CC-4S. Readings were taken from all the gages at each load increment.

The maximum dynamic load to be applied during the fatigue tests was controlled by the deflections obtained under the first static load test and under additional static load tests performed at frequent intervals. Dur- the initial stages of each fatigue test, the dynamic deflections of each span could not be made simultaneously equal to the corresponding controlling static deflections. In this case, the dynamic load was taken so that the smaller dynamic deflection under one of the two load points was equal to the corresponding controlling static deflection. The dynamic deflection at the other load point was therefore in excess of its controlling static deflection during the increment of applied cycles of fatigue loading. However, the controlling static deflections, corresponding to equal maximum static loads, also increased rapidly during the initial stages of each test due to bond failure between slab and beam as well as other causes. Therefore, the procedure followed was not considered unconservative.

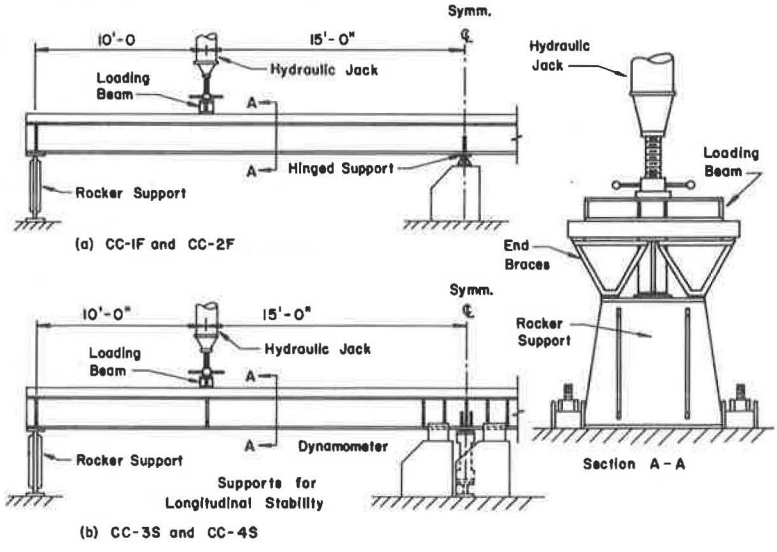

Figure 6. Test setup for all fatigue tests.

The maximum dynamic load was always less than the maximum static load because of the dynamic effect. For beams CC-1F and CC-2F the dynamic load correction was usually from 1 to 2.5 kips at each load point. In all the beam tests the higher value was associated with the initial 10 to 20 percent of the total number of cycles applied to the beam, except for beam CC-1F where a value of 6.5 kips was reached midway through the test.

The minimum dynamic load varied from 3.5 to 7.5 kips for beams CC-1F and CC-2F and from 2.0 to 4.0 kips for beams CC-3S and CC-4S. The lower values tended to be associated with the initial stages of the test. The minimum load was the smallest that could be applied without separation of the beam and loading jack throughout the fatigue testing period.

It was apparent that connectors were failing in beam CC-1F after 500,000 cycles of load application. This was more serious in the east span where the resulting loss of stiffness caused a large difference in the deflections of the two spans at approximately 1,100,000 cycles. If the fatigue test of beam CC-1F was to continue to 2,000,000 cycles some means of preventing the large differences in stiffness between the two spans was necessary. Therefore, a clamp was installed in the east span approximately at the inflection point so that greater frictional resistance could be developed between the slab and the steel beam. The clamp consisted of two steel plates welded to the underside of the top flange of the steel beam on opposite sides of the web and then bolted through the slab to another steel plate on the top of the slab. Even with this reinforcement, the fatigue test of beam CC-1F was stopped short of 2,000,000 cycles of load application due to accelerated failures of connectors in the west span. The clamp was installed at 1,074,900 cycles and removed at 1,375,500 cycles after deflections in both spans had again stabilized.

After completion of each fatigue test, the continuous beam was tested to its static ultimate strength (12). After testing the concrete slab was removed from the steel beam in the vicinity of the exterior supports, throughout the negative moment region, and from the positive moment regions near the points of contra-flexture. Photographs were then taken of the connector failures and cracked connectors. Also, each connector in these regions was bent at least 45 deg with a sledge to ascertain whether fatigue cracks were present. Several connectors fractured during this process. The visual inspection and bending test were used as a verification of the information obtained from the electrical resistance strain gages placed under the studs as follows: (a) if a connector was seen to be completely fractured when the steel beam was exposed or was removed during the 45-deg bending test, its strain-cycle curve (Fig. 12, for example) was examined to ascertain its cycle life—the number of cycles corresponding to a sharp reduction in strain reading was taken as the cycle life of the connector (4, 5); (b) if a connector did not fracture from the flange during the bending test but a fatigue crack was visually present, its cycle life was taken as the total number of cycles applied to the specimen; (c) if a connector did not fracture and if no fatigue cracks were visible, its cycle life was considered greater than the total number of cycles applied to the specimen.

TEST RESULTS

Each continuous composite beam except CC-1F was subjected to at least the desired amount of cyclic loading: 1,906,900 cycles of load were applied to beam CC-1F and 2,079,000 cycles of load were applied to beam CC-2F. Beams CC-3S and CC-4S each had 500,000 cycles of load applied. As previously stated, it was observed during testing of beam CC-1F, that studs in the east span were beginning to fail in fatigue at about 500,000 cycles and that they were continuously deteriorating with increasing cycles of load application. The installation of a clamp in the east span allowed additional cycles of load to be applied but accelerated the deterioration of the studs in the west span. The deterioration of the studs in beam CC-1F eventually progressed to the point where the fatigue test was stopped short of the desired 2,000,000 cycles so that a sufficient number of connectors would be left to develop the ultimate load capacity of the beam.

Deformation of the Continuous Beams

Deflection under the load point of each beam was measured at intervals throughout the fatigue testing period. Figure 7 summarizes the load-deflection characteristics of the east spans of beams CC-1F and CC-2F. The curves are plotted for the start of testing, for two intermediate cycle levels, and at the end of testing. For comparison, the theoretical curves for complete interaction and no interaction are shown. Two curves for complete interaction are shown for beam CC-1F. The steeper curve assumes complete interaction throughout the beam (same as for beam CC-2F) and the other assumes complete interaction only in the regions containing studs.

It was apparent after completion of the test program that a small but varying amount of support settlement had occurred during all of the tests partly because of the presence of lead shims at the interior supports. The deflections of the supports were not measured in any of the tests. Some inelastic support settlement occurred during the initial zero-to-maximum static loading of each beam at the start of fatigue testing. For this reason, the 0 cycle curves (Fig. 7) are plotted so that the unloading curve passes through the origin. Subsequent zero-to-maximum load-deflection curves therefore show only the effect of further inelastic behavior due to support settlement and other causes as fatigue testing was continued.

Strain Measurements in the Continuous Beams

Strains measured with the electrical resistance strain gages and strains measured using mechanical strain gage points, were used to obtain the distributions of strain throughout the depth of the four continuous beams in both the positive and the negative moment regions. Typical strain distributions in the positive moment regions are shown in Figure 8a, which shows the distribution of strains corresponding to a static load of 60 kips. Omitting connectors in the negative moment region of beam CC-1F apparently has little effect on the distribution of strains in the positive moment regions. Similar behavior has been reported (7). It is also apparent that the difference in reinforce-

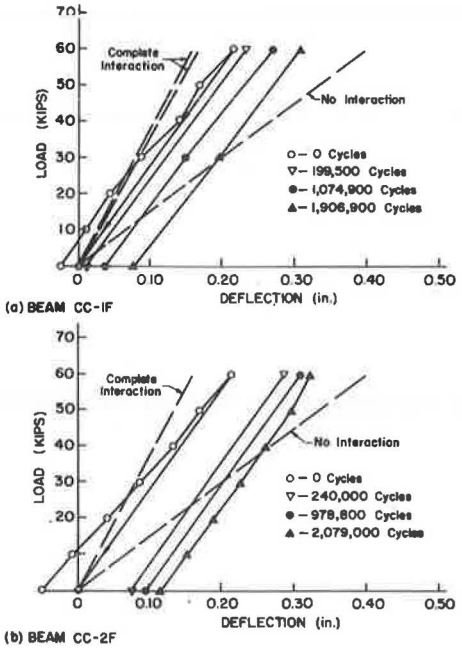

Figure 7. Load-deflection curves for beams CC-1F and CC-2F.

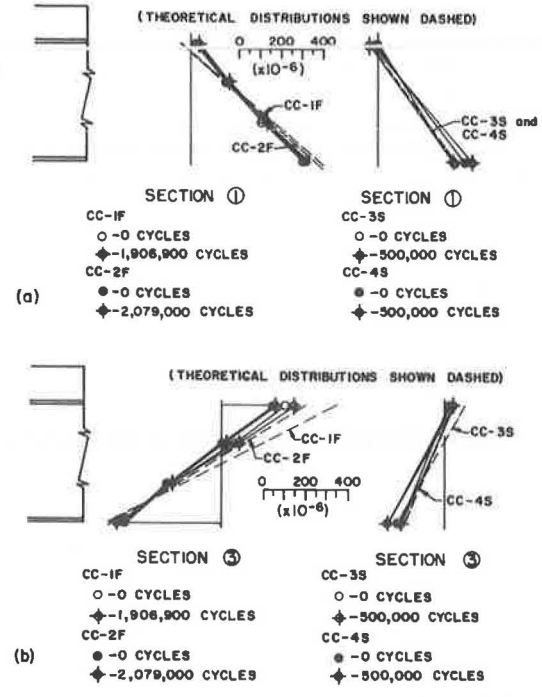

Figure 8. Typical strain distributions in positive and negative moment regions.

ment and placement of studs in beams CC-3S and CC-4S had no significant effect on the distribution of strains in the positive moment regions of these beams.

Similar comparisons of strains are made in Figure 8b for a typical section in the negative moment region of the four continuous beams. The comparison is again made for a static load of 60 kips. Even though beam CC-1F had no shear connectors in the negative moment region, the slab and reinforcement had some effect on the strains in this region. Also, the effect of the large amount of longitudinal reinforcement in beams CC-3S and CC-4S can be observed by comparing the strain distribution for all four beams.

Figure 9a compares the location of the neutral axis as a function of applied cycles for typical sections in the positive moment regions of beams CC-1F and CC-2F. Figure 9b makes a similar comparison for beams CC-3S and CC-4S. The number of applications of load had only a small effect on the flexural behavior in the positive moment regions of all four beams.

Figure 10 shows the location of the neutral axis as a function of the applied cycles for typical sections in the negative moment regions. The slab had cracked in all four beams under the initial application of load and that additional applications of load had only a small effect on the stresses in the steel beams.

Strain Measurements Near Stud Connectors

Strain gages were placed on the bottom of the upper beam flange to obtain strain-cycle data from the stud shear connectors in three regions of each beam as follows: (a) near the exterior supports, (b) in the positive moment region adjacent to the points of contraflexure, and (c) in the negative moment regions.

The strain measurements were taken during the static tests made at intervals during the fatigue tests. The strains obtained at the maximum load were plotted as a function of the applied cycles. Typical results are shown in Figures 11 and 12. Each figure shows schematically a portion of two steel beams below a strain versus cycle plot for certain studs on the steel beam. The studs are identified as follows:

1. Open circles represent studs from which strain versus cycle data were obtained, studs which were examined visually following fatigue testing, or both.

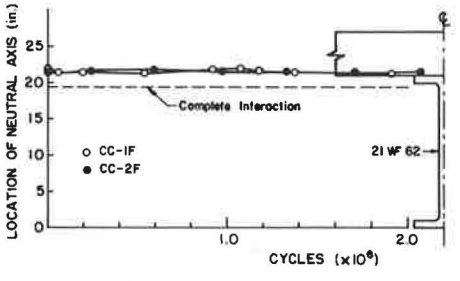

(a) BEAMS CC-1F and CC-2F (SECTION 1)

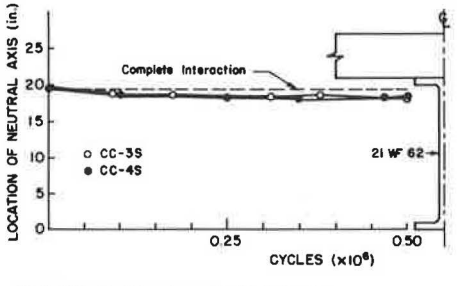

(b) BEAMS CC-3S and CC-4S (SECTION 1)

Figure 9. Location of the neutral axis in the positive moment regions.

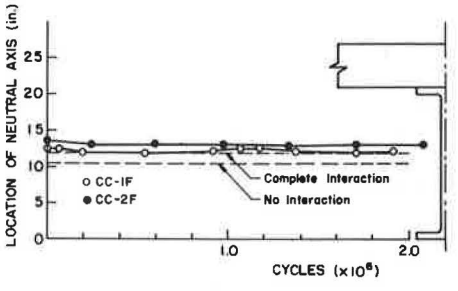

(a) BEAMS CC-1F and CC-2F (SECTION 3)

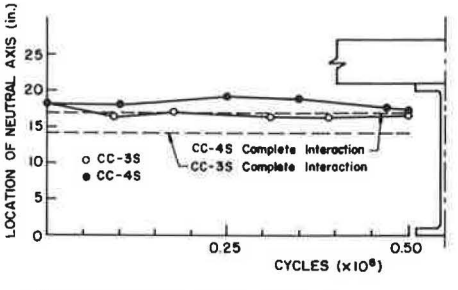

(b) BEAM CC-3S and CC-4S (SECTION 3)

Figure 10. Location of the neutral axis in the negative moment regions.

2. Shaded circles represent studs for which the strain versus cycle curves are plotted immediately above.
3. Circles with strokes through them represent studs which had failed during fatigue testing as evidenced by their separation from the steel beam either before or during the 45-deg bending test.

Figure 11 illustrates the response observed over the west exterior supports of three of the four beams. The behavior over the east supports was similar. It is apparent that, for beams CC-1F and CC-2F, as fatigue loading was applied to the composite sections, the strains in the flange increased due to increasing flange distortion, indicating that greater load was being carried by the connectors as bond was lost. The strains then leveled out after a few thousand cycles of load application and remained reasonably uniform throughout the remaining portion of the test. The soundness of the connectors over the supports of beam CC-1F is illustrated in Figure 13 where the photograph, taken after fatigue testing, shows all to be sound even after bending 45 deg. It can also be observed from Figure 11 that the connector failures in beam CC-4S were not apparent from the strain measurements taken near the studs. However, after the slab was removed, the studs were removed from the beam during the bending test. This result was expected in beam CC-4S since the studs in this region were subjected to a high range of shear load in excess of the allowable load range (see Table 1). All studs over the support in beam CC-4S were removed with one tap of a sledge hammer, whereas the three failed studs in beam CC-3S were bent nearly 45 deg before failure. No strain-cycle data were obtained in this region of beam CC-3S.

Figure 12 illustrates the type of response observed near the east inflection points of the four beams. As was noted for the regions over the supports, strain increased as the bond was broken and greater load was transferred to the connectors. In addition, it is significant that the strains measured in beam CC-1F were nearly twice as great as the strains measured in beam CC-2F, because no connectors were provided in the negative moment region of CC-1F and the force in the longitudinal reinforcing steel in that region was being carried by the adjacent connectors in the positive moment region.

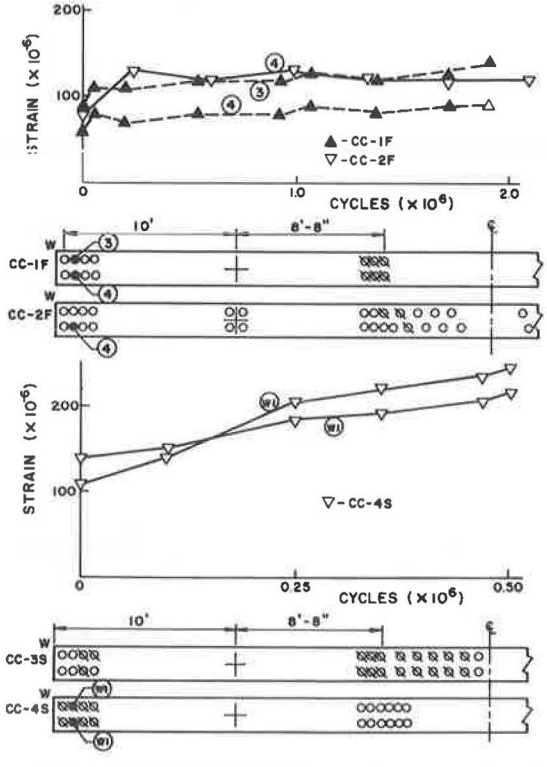

Figure 11. Typical local strain readings vs cycles of the ends of the test beams.

As the fatigue loading continued, the strains in the flange of beam CC-1F remained reasonably stable for at least 500,000 cycles. Thereafter, the strains began to decrease as a fatigue crack started to propagate through the base of the stud shear connector (5). This decrease was particularly severe in the east span of beam CC-1F and was nearly the same for all three sets of instrumented studs in this region. The failure of connectors near the point of contraflexure in the east span was rapid.

Figure 12 also shows that virtually all of the studs examined in the negative moment region and near the inflection points of beam CC-3S had failed. These studs were all removed easily during the bending test. This behavior was expected because of the higher than allowable load range in the negative moment region. Evidently, as studs in this region began

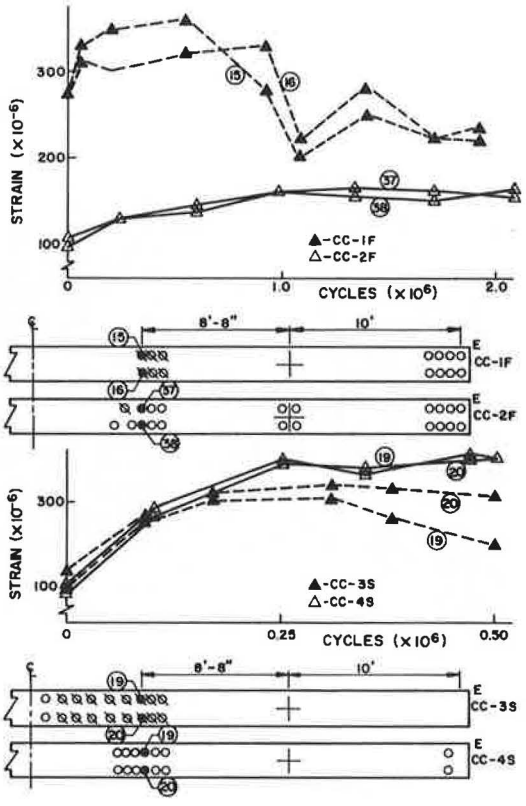

Figure 12. Local strain readings vs cycles at the east inflection points of the test beams.

Figure 13. Studs at the end of beam CC-1F after fatigue testing.

to fracture, load was transferred to the studs in the positive moment region closer to the inflection points thus accelerating their rate of failure.

The process of load transfer becomes even more apparent in Figure 14 when similar studs in the west span of beam CC-4S are examined. The studs between the load points and the inflection points were considerably overloaded (see Table 1). Therefore, a transfer of load to both of the exterior support regions and to the negative moment region would take place as studs began to fracture. Sufficient capacity existed in the negative moment region to stop complete stud failure near the inflection points. Since no excess capacity existed over the supports, load transfer probably accelerated the stud failures in that region. The response of studs in the west negative moment region of beam CC-2F is also illustrated in Figure 14. A continuous increase in the apparent strain was noted for the first few hundred thousand cycles as the bond was broken and the slab cracking progressed. In this beam, three of the studs fractured after the slab was removed and the studs bent 45 deg. All six studs examined in beam CC-1F near the inflection point were fractured.

The studs near the east inflection points of beam CC-1F are shown in Figure 15. The inflection point passes through the two circular craters at the bottom of the photo which were left by the failure of studs 15 (left) and 16 (right). These studs remained embedded in the portion of concrete slab which was removed. Studs 17 and 19 (left) and 18 and 20 (right) are shown beside their former positions after they were removed by hand. Since these studs were nearly completely fractured from the beam after the slab was removed, it is probable that the high strain readings observed at the end of the test were caused by the doweling of the failed stud in the rather deep crater that was taken from the beam flange. Figure 16 is a typical view of the fracture surface of one of these studs showing the fatigue fracture surfaces.

ANALYSIS OF TEST RESULTS

Stresses and Bending Moments in Continuous Composite Beams

Figures 9 and 10 show that reasonably good agreement can be obtained by assuming that all beam sections, including the negative moment region of beam CC-1F, have com-

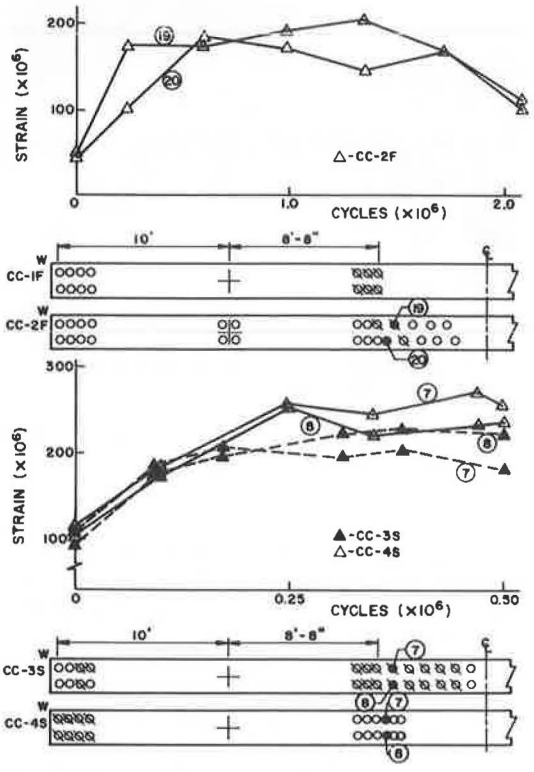

Figure 14. Local strain readings vs cycles in the negative moment regions of the test beams.

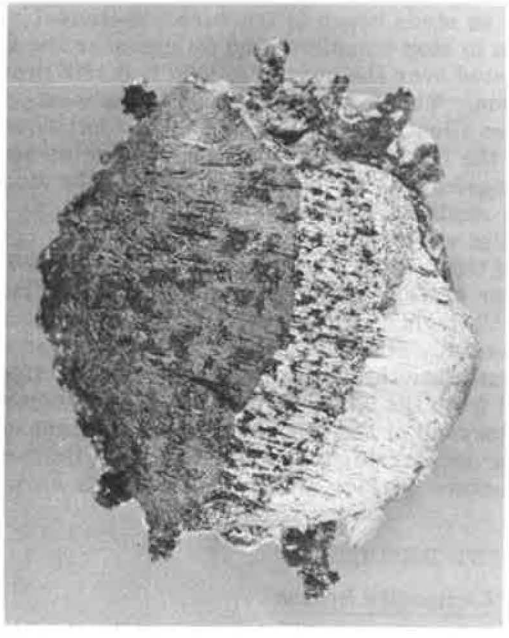

Figure 16. Fracture surface of a stud at the east inflection point of beam CC-1F after fatigue testing.

Figure 15. Studs at the east inflection point of beam CC-1F after fatigue testing.

plete interaction. It is apparent that the steel beam section of beam CC-1F is interacting with the longitudinal reinforcement in the negative moment region. This behavior should be expected since considerable tensile force will be developed in the longitudinal steel due to the rotation of the beam cross sections at each inflection point. Since no shear transfer can take place between the slab and the beam after bond has been broken (except for frictional forces) flexural conformance cannot exist in the negative moment region of beam CC-1F. A higher degree of flexural conformity was present in beam CC-2F, but was less than the assumption of complete interaction would require.

Slab Force Resisted by Shear Connection

In composite beams, the degree of interaction and flexural conformance is determined by the amount of slip between the concrete slab and the steel beam. A high degree of flexural conformance can be maintained only if sufficient shear connection is provided to minimize the slip. Interaction and flexural conformance are of particular interest in the negative moment regions of continuous composite beams. To help evaluate the degree of interaction in

beams CC-1F and CC-2F, the force in the slab at the inflection points and near the center support was computed from the measured strains in the steel beams. Computations of the tensile force in the slab based on the strain data from the reinforcing steel over the support were not as reliable because of the influence of moment gradient and slab cracking. Figure 17 shows the computed slab forces near the center support of beams CC-1F and CC-2F as a function of the applied cycles of load. The theoretical tensile slab force based on three simplifying assumptions is shown for comparison. Assumption (c) in Figure 17 considers the tensile force in the longitudinal reinforcement computed from the rotations at the inflection points.

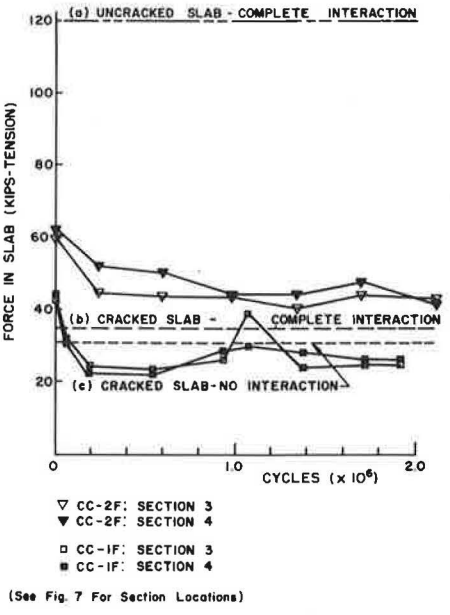

Figure 17. Slab force near the center support of beams CC-1F and CC-2F.

The slab force over the support of both beams rapidly decreased during the first 200,000 cycles of loading. This was probably due to loss of interaction as bond was destroyed, as well as slab cracking. In beam CC-1F, the initial slab force (force in the longitudinal reinforcing) was nearly equal to the theoretical value for a cracked section with complete interaction, but rapidly decreased to a level somewhat below the predicted value, assumption (c). However it was observed from other data that at the inflection points of beam CC-1F the slab force was virtually as predicted at least up to the observed initial failure of connectors. Since frictional forces can account for the small difference between the measured and predicted force near the support, it is apparent that, neglecting friction, the slab force is nearly uniform over the entire negative moment region when no connectors are placed in that region.

The slab force in beam CC-2F maintained a level in the region near the interior support somewhat greater than that in beam CC-1F. Because of the presence of shear connectors, a higher initial slab force was observed (Fig. 17) until the slab was fully cracked. The slab force decreased in both spans of beam CC-2F at about the same rate. The force approximately stabilized at a value somewhat above the predicted value, assumption (b), after about 200,000 cycles. Other data indicated that at the inflection points of beam CC-2F the slab force approached zero, which flexural conformance would require. It is obvious, then, that for beam CC-2F shear transfer was taking place between the slab in the negative moment region and the steel beam as a result of the stud shear connection in that region.

Similar behavior was observed in the negative moment regions of beams CC-3S and CC-4S; however, the slab forces were substantially greater in these two beams because of the increased amounts of longitudinal reinforcing steel. The degree of interaction was also somewhat greater because of the greater number of shear connectors in the negative moment region.

The effect of stud failures near the inflection points of beam CC-1F on the slab forces at the center support is also shown in Figure 17. The slab forces were rapidly changing at about 1,000,000 cycles. The clamp which was in place from 1,074,900 cycles to 1,375,500 cycles resulted in a readjustment of the slab forces so that they were again reasonably uniform.

It is apparent from the fatigue behavior of the four test beams and the comparison (Fig. 17) that shear connectors are required to resist the slab force in the negative moment region of all continuous composite beams which have continuous longitudinal reinforcement.

Forces on Stud Connectors

It was also of interest to examine the forces to which the shear connectors were subjected during the progress of the tests. Of particular interest were those connectors at the ends of the beams, in the positive moment regions adjacent to the points of contraflexure and in the negative moment region. Bond failure between the slab and the beam as well as slab cracking took place in the negative moment region (Fig. 17). The slab force necessarily had to be resisted by the connectors alone when they were present. In the end portions of each beam, bond failure started at the end of the member and progressed toward the load points. In the positive moment regions adjacent to the points of contraflexure, bond failure progressed from the points of contraflexure toward the load points.

The average force per connector was computed as the compressive force in the slab at a strain gage location divided by the number of connectors between that location and the end of the beam or the point of contraflexure, whichever was applicable. Table 5 summarizes the forces on the studs in the west spans of each beam at various cycles of load application. The forces in the east spans were similar. The applied load was 60^k for beams CC-1F, CC-2F, and CC-3S, and 70^k for beam CC-4S. A comparison is made between the shear forces computed from strain data with the values of shear force computed according to elastic theory for horizontal shear. In general, the agreement could be considered good, taking into account the assumptions made.

In beam CC-1F, since no connectors were provided in the negative moment region to resist the slab force, it was resisted only by the shear connectors in the positive moment regions adjacent to the points of contraflexure. The test showed that at least three pairs of studs adjacent to the points of contraflexure were carrying the additional force. Qualitative strain-cycle measurements were not taken on other studs in these regions, so it was not known how many other studs adjacent to the points of contraflexure actually resisted the additional slab force transmitted by the longitudinal slab steel in the negative moment region. If one assumes this additional force to be averaged over all the connectors between the load point and the point of contraflexure, the shear load varied from approximately 5.70 to 5.90 kips per stud as shown in Table 5. If only half the connectors were assumed to carry this load, then they would be subjected to an average shear of about 7 kips per stud.

Figure 18 compares the design cumulative resistance of the shear connectors in beam CC-1F and CC-2F with the measured slab force at various locations along the beams. The comparison is made at 2,000,000 cycles with a load of 60 kips. It is apparent that connectors in beam CC-2F were subjected to forces that very closely correlated with their design resistance. Figure 18 also shows that in the negative moment region of

TABLE 5

TYPICAL FORCES ON STUD SHEAR CONNECTORS

Location	CC-1F			CC-2F			CC-3S			CC-4S		
	Cycles ($\times 10^6$)	Test (k)	Theor. (k)	Cycles ($\times 10^6$)	Test (k)	Theor. (k)	Cycles ($\times 10^6$)	Test (k)	Theor. (k)	Cycles ($\times 10^6$)	Test (k)	Theor. (k)
End of beam positive moment	0	4.50	4.40	0	4.47	4.40	0	5.44	5.40	0	6.08	6.10
	0.539	4.44	4.40	0.597	4.61	4.40	0.310	5.00	5.40	0.348	5.80	6.10
	1.075	4.47	4.40	0.979	4.49	4.40	0.500	4.84	5.40	0.500	5.90	6.10
	1.376	4.51	4.40	1.335	4.51	4.40						
	1.907	4.44	4.40	2.079	4.55	4.40						
Interior positive moment	0	5.82	5.40[a]	0	5.27	4.40	0	5.85	5.20	0	7.08	6.40
	0.539	5.70	5.40	0.597	5.32	4.40	0.310	5.38	5.20	0.348	6.75	6.40
	1.075	5.94	5.40	0.979	5.20	4.40	0.500	5.19	5.20	0.500	6.86	6.40
	1.376	5.72	5.40	1.335	5.20	4.40						
	1.907	5.68	5.40	2.079	5.57	4.40						
Negative moment				0	5.11	4.40	0	6.67	6.20	0	3.46	4.30
				0.597	3.32	4.40	0.310	4.96	6.20	0.348	3.95	4.30
				0.979	3.19	4.40	0.500	5.44	6.20	0.500	3.20	4.30
				1.335	3.10	4.40						
				2.079	2.12	4.40						

[a]Force from longitudinal reinforcement in negative moment region included and distributed over all studs in the interior moment region.

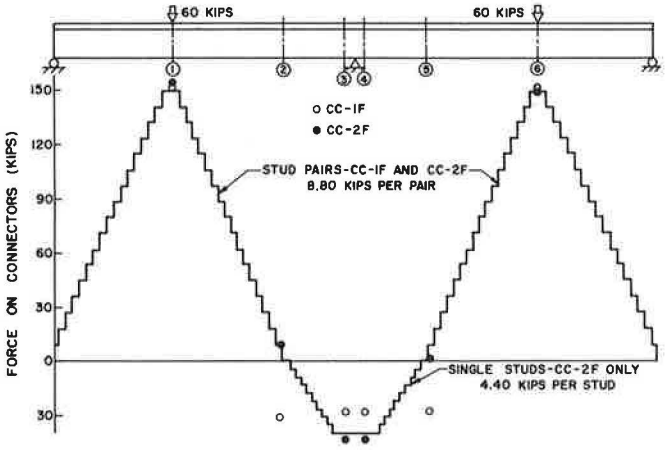

Figure 18. Cumulative resistance of stud shear connectors for beams CC-1F and CC-2F at 2,000,000 cycles.

beam CC-2F the tensile force in the slab was being adequately transferred into the beam by the shear connectors. At the points of contraflexure little slab force was present, confirming that the connectors in the negative moment region were effective. Similar behavior was observed in beams CC-3S and CC-4S.

In beam CC-1F, this was not the case. The slab force was approximately the same at the points of contraflexure and near the center support. This reconfirms the previous discussion on the behavior in the negative moment region. It is apparent that the longitudinal slab reinforcing was acting like tendons in an unbonded posttensioned beam, with the reinforcing being anchored in the region of the inflection points. Consequently, the studs near the inflection points were subjected to shear forces considerably higher than those used in the designs. This undoubtedly contributed to the early failure of those shear connectors in beam CC-1F.

Fatigue Strength of Stud Shear Connectors

It is realized that the method of detecting connector failure is not exact but it is believed to give conservative results. Table 6 summarizes all the test data to show the cycle life for the connectors in the five regions of interest for each test beam. Also

TABLE 6

SUMMARY OF CONNECTOR CYCLE LIVES

Location	CC-1F			CC-2F			CC-3S			CC-4S		
	Cycle Life ($\times 10^6$)	Stress Range (ksi)	Fail[a] Ratio	Cycle Life ($\times 10^6$)	Stress Range (ksi)	Fail[a] Ratio	Cycle Life ($\times 10^6$)	Stress Range (ksi)	Fail[a] Ratio	Cycle Life ($\times 10^6$)	Stress Range (ksi)	Fail[a] Ratio
W. end pos. moment	2.00+	10.15	0	2.00+	10.30	0	0.50	11.65	0.38	0.50	13.40	1.00
E. end pos. moment	2.00+	10.75	0	2.00+	10.00	0	—	11.40	—	0.50	13.50	—
W. interior pos. moment	1.00	13.01[b]	1.00	2.00	11.80	0.17	0.50	13.00	1.00	0.50+	15.50	0
E. interior pos. moment	0.50	12.72[b]	1.00	2.00+	10.90	0	0.50	12.70	1.00	0.50+	14.75	0
Negative moment	—	—	—	2.00	9.60	0.17	0.50	12.80	0.83	0.50+	8.00	0

[a] Ratio of number of studs failed to number of studs examined.

[b] The force in the negative reinforcement was distributed over all the studs in the interior positive moment regions; distribution of force over one-half the studs would increase the stress ranges to 15.33 and 14.70 ksi, respectively, for the W. and E. interior positive moment regions.

given is the average stress on the connectors in a given region during the indicated cycle life. Failures were observed in all four test beams.

The test data summarized in Table 6 were compared in Figure 19 with the previously developed S-N curve (3). Each failure point (shaded circle) represents the average stress versus observed cycle life, for from 6 to 24 studs. Where no failures were observed the points were ploted as runouts (open circle with arrow). Pushout tests provide a lower bound of the fatigue strength (3). Since the mean S-N curve (Fig. 10, 3) was based on pushout tests, these beam test results were expected to exhibit slightly greater cycle lives. Most of the test results in Figure 19 verify this behavior since they lie between the mean curve and the upper limit of dispersion. Except for one failure point representing the early failures near the east inflection point of beam CC-1F, each failure point lying below the mean curve in Figure 19 represents failures detected only by the bending test. No failures were apparent from the flange distortion gage readings for these studs. Thus, these points represent a conservative estimate of cycle life.

Comparison of Beam Performance

The four continuous composite beams provide several direct comparisons of beam performance. Two major variables were evaluated: (a) the placement of connectors in the negative moment region; and (b) the effect of increasing the amount of longitudinal steel in the negative moment region.

The placement of connectors in the negative moment regions of beams CC-2F, CC-3S, and CC-4S provided better flexural conformance, better dynamic response of the beam, and more uniform beam behavior. The performance of beam CC-1F was decidedly poor. Premature fatigue failures were detected near the points of contraflexure, and the general response of the beam to cyclic loading was very poor. The two spans of this beam were observed to behave differently under dynamic load. Since the dynamic behavior of CC-2F was considerably improved, this was undoubtedly due to the presence of shear connectors in the negative moment region of beam CC-2F, since all other aspects of CC-1F and CC-2F were identical.

The slab cracking patterns in beams CC-1F and CC-2F also differed appreciably. In beam CC-1F, the cracks were of about equal width throughout the negative moment region, confirming that the force in the longitudinal reinforcement was reasonably uniform throughout that region. Although beam CC-2F had connectors designed to transmit the force in the longitudinal reinforcement, they were not continuous throughout the negative moment region partly because only a few were required but mainly because it was desirable to shift them toward the points of contraflexure in order to prevent a premature fatigue failure in the beam flange over the center support. As a result,

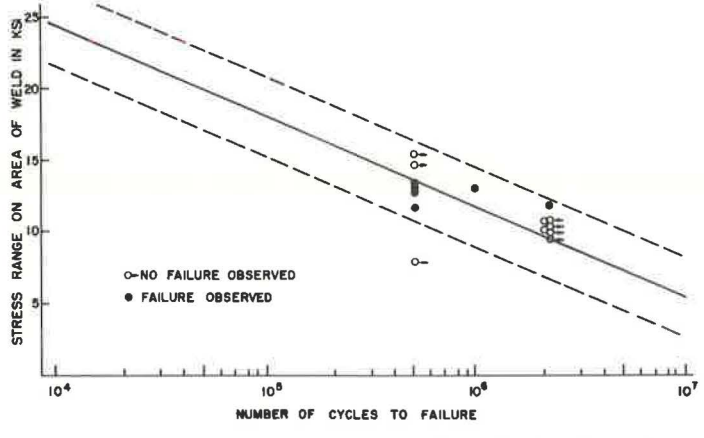

Figure 19. Semilog plot of stress range vs cycle life for all test beams.

large cracks occurred in the short length in which the connectors were omitted. As bond was destroyed and the slab force was transferred to the connectors in the negative moment region, the crack widths decreased somewhat as additional smaller cracks appeared closer to the inflection points. In both beams CC-1F and CC-2F, the maximum crack widths exceeded the suggested limits (8) for cracks in reinforced concrete bridges at the service load level.

Beams CC-3S and CC-4S had substantially more longitudinal reinforcement in the negative moment region. This additional reinforcement greatly increased the flexural conformance of the composite beams. In addition, slab cracking behavior was greatly improved over that of beams CC-1F and CC-2F. There was not much difference in the behavior of beams CC-3S and CC-4S with respect to dynamic response, flexural conformance, and crack width and distribution. Hence the larger increase in longitudinal reinforcement in beam CC-4S provided virtually no improvement in behavior over that of beam CC-3S.

Comparison of Test Results With Design Recommendations

It has been suggested that shear connectors are needed in the negative moment regions to provide resistance to the force developed in the reinforcing steel (3). Also, elastic theory assuming complete interaction was recommended to evaluate the horizontal shear resisted by the shear connection. The present study has confirmed these recommendations. It has shown clearly that shear connectors are required to resist the force developed in continuous longitudinal reinforcement steel in the negative moment regions. When they are omitted, the response of the structure will be poor and fatigue failure of connectors adjacent to the points of contraflexure will occur at a substantially lower number of cycles than that assumed in the design. This study also confirmed that elastic theory can be used to evaluate the horizontal shear transferred by the shear connectors. Only the cracked section of the concrete slab is effective. Thus, the statical moment of the composite section need only consider the longitudinal reinforcing steel in the slab. All longitudinal reinforcing steel in the slab cross section was observed to be effective in these tests. It would appear, then, that all longitudinal reinforcement should be taken into account when ascertaining the magnitude of the slab force which must be resisted, at least up to the width-to-depth ratio used in this study.

CONCLUSIONS

The following conclusions were drawn from an anlaysis of the test results:

1. Shear connectors are required to resist the force in the longitudinal slab reinforcement in the negative moment regions of continuous composite beams. The amount of shear connection required depends upon the percentage of longitudinal reinforcing steel in that region.
2. More longitudinal reinforcement in the negative moment regions of continuous composite beams than presently allowed by the AASHO Specifications appears to be desirable in order to control the number and widths of slab cracks as well as to improve interaction and flexural conformance in that region. It was evident from the test results that this will also improve the deflection characteristic and overall structural behavior of the continuous composite beam under dynamic loads.
3. Further study is required to evaluate the effects of stud placement, cover plates prestressing and haunching in the negative moment regions of continuous composite beams, as well as to determine the optimum reinforcement required for adequate crack control.

ACKNOWLEDGMENTS

The study described in this report was part of an investigation on composite beams that was conducted at Fritz Engineering Laboratory, Department of Civil Engineering, Lehigh University. L. S. Beedle is Director of the Laboratory. The project was financed by the New York Department of Transportation; the U. S. Department of Transportation, Bureau of Public Roads; Nelson Stud Division of Gregory Industries,

Inc.; KSM Products Division of Omark Industries Inc.; Tru-Weld Division of Tru-Fit Screw Products Inc.; and Lehigh University.

The writers are indebted to R. G. Slutter for his advice and help in the planning and conduct of these tests. Sincere thanks are also due Noriaki Yoshida and James O. Armacost III for assistance in the conduct of several of the tests and for aid in reducing and analyzing the test data; to K. R. Harpel and C. F. Hittinger for their work in preparing the test setup and instrumentation; and to R. N. Sopko for preparing the figures.

REFERENCES

1. AASHO. Standard Specifications for Highway Bridges. Ninth Edition, Washington, D.C., 1965.
2. Viest, I. M., Fountain, R. S., and Siess, C. P. Development of the New AASHO Specifications for Composite Steel and Concrete Bridges. HRB Bull. 174, p. 1-17, 1958.
3. Slutter, R. G., and Fisher, J. W. Fatigue Strength of Shear Connectors, Highway Research Record 147, p. 65-88, 1966.
4. Toprac, A. A. Fatigue Strength of ¾-Inch Stud Shear Connectors, Highway Research Record 103, p. 53-77, 1965.
5. King, D.C., Slutter, R. G., and Driscoll, G. C. Fatigue Strength of ½-Inch Diameter Stud Shear Connectors, Highway Research Record 103, p. 78-106, 1965.
6. Siess, C. P., Viest, I. M., and Newmark, N. M. Studies of Slab and Beam Highway Bridges: Part III, Small Scale Tests of Shear Connectors and Composite T-Beams. Univ. of Illinois Engineering Experiment Station, Bull. 396, 1952.
7. Siess, C. P., and Viest, I. M. Studies of Slab and Beam Highway Bridges: V. Tests of Continuous Right I-Beam Bridges. Bull. 416, Univ. of Illinois Engineering Experimant Station, 1953.
8. U.S. Department of Commerce, Bureau of Public Roads. Tentative Criteria for Ultimate Strength Design of Reinforced Concrete Highway Bridges, 1966.
9. Slutter, R. G., and Driscoll, G. C. Flexural Strength of Steel-Concrete Composite Beams. Jour. Structural Division ASCE, Vol. 91, No. ST2, April 1965.
10. Barnard, P. R., and Johnson, R. P. Plastic Behavior of Continuous Composite Beams. Proc. Institution of Civil Engineers, Vol. 32, p. 161-179, Oct. 1965.
11. Johnson, R. P., VanDalen, K., and Kemp, A. R. Ultimate Strength of Continuous Composite Beams. Progress Report, British Constructional Steelwork Association Conference, Sept. 1966.
12. Daniels, J. H., and Fisher, J. W. Static Behavior of Continuous Composite Beams. Fritz Engineering Laboratory Report 324.2, March 1967.
13. Recommendations for the Design and Construction of Composite Beams and Girders for Buildings. Appendix C—Welding and Inspection of Stud Shear Connectors, Report of the Joint ASCE-ACE Committee on Composite Construction, 1966.